63, 4, pp. 889–902, Warsaw 2025 https://doi.org/10.15632/jtam-pl/207524

EXPERIMENTAL INVESTIGATION OF THE LONG-TERM MECHANICAL BEHAVIOR OF MUDSTONE UNDER VARYING WATER CONTENTS

Zhuangen QIN

China Anneng Group Third Engineering Bureau Co.Ltd., Chengdu, China qinzexx@sina.com

This study presents a series of uniaxial compression and creep tests designed to elucidate the long-term mechanical properties of mudstone subjected to different water content conditions. The results demonstrate that water content exerts a significant influence on the short-term strength, elastic modulus, and creep response of mudstone. Specifically, the uniaxial compressive strength and elastic modulus exhibit an exponential decrease with increasing water content. Furthermore, the creep behavior of mudstone is markedly affected by water content. A creep damage model, integrating the Burgers model with water-induced and creep-induced damage variables, is proposed.

Keywords: mudstone; water content; creep; damage variable; creep damage model.



Articles in JTAM are published under Creative Commons Attribution 4.0 International. Unported License https://creativecommons.org/licenses/by/4.0/deed.en. By submitting an article for publication, the authors consent to the grant of the said license.

1. Introduction

Mudstone, a widely distributed sedimentary rock, plays a vital role in geotechnical engineering applications, including slope stabilization, tunneling, and foundation design. Its mechanical behavior is notably sensitive to environmental factors, particularly water content. Variations in water content can induce substantial alterations in mudstone's strength, deformability, and long-term stability. For instance, in slope engineering, cyclical wetting-drying processes resulting from rainfall or groundwater fluctuations may trigger swelling, softening, and potentially catastrophic failure of mudstone slopes (Qi et al., 2024; Yu et al., 2024). Similarly, in underground excavations, water infiltration can accelerate creep deformation, thereby jeopardizing structural integrity (Li et al., 2023; Wang et al., 2021). This is especially relevant in areas prone to landslides, such as the Three Gorges Reservoir Area in China, where the purple mudstone of the Middle Triassic Badong Formation is particularly susceptible to creep-related failures (Wang et al., 2021). Despite its practical relevance, the long-term mechanical response of mudstone under variable water conditions remains incompletely understood, particularly in scenarios involving sustained loads, such as dam foundations or deep tunnels. A thorough understanding of these mechanisms is essential for optimizing engineering designs, mitigating risks, and ensuring the long-term safety of infrastructure projects. This study addresses this knowledge gap by systematically investigating the influence of water content on both the short-term and long-term mechanical properties of mudstone.

Numerous investigations have explored the relationship between water content and the mechanical behavior of mudstone (Chen et al., 2022; Liu et al., 2021; Shao et al., 2024; Zheng et al., 2024). These studies have highlighted the critical role of water in weakening mudstone's mechanical properties. For instance, several studies have focused on the impact of water content on the unconfined compressive strength (UCS) and Young's modulus, demonstrating a marked decrease in these parameters with increasing water (Chen et al., 2022; Gao et al., 2023). Microstructural analyses, using techniques like scanning electron microscopy (SEM), have further revealed that

water intrusion leads to changes in cementation, compaction, and pore size distribution within the mudstone matrix, ultimately contributing to the degradation of its mechanical properties (Gao *et al.*, 2023; Shao *et al.*, 2024; Zheng *et al.*, 2024).

The time-dependent behavior of mudstone under varying water conditions has also been a subject of extensive research. Creep tests conducted under different confining pressures and water contents have demonstrated that water significantly alters the creep characteristics of mudstone (Li et al., 2023; Wang et al., 2021). Sawatsubashi et al. (2021) found that immersion-induced creep deformation is influenced by both initial water content and shear stress, with higher initial water content leading to increased creep deformation. Moreover, cyclic wetting-drying tests have shown that repeated cycles exacerbate the deterioration of mudstone's mechanical properties, leading to a transition from brittle to ductile behavior and a reduction in shear strength (Yu et al., 2024; Yang et al., 2022). The damage mechanisms associated with these cycles involve swelling and shrinkage of clay minerals, dissolution of soluble minerals, and the development of microcracks (Yang et al., 2022; Yu et al., 2024).

Constitutive models have been developed to capture the complex behavior of mudstone under varying water and stress conditions. Wang et al. (2020) proposed a nonlinear disturbance creep damage model based on the Burgers model to account for the influence of cyclic disturbance loads on mudstone creep. Ma et al. (2018) developed a new shear rheological model to describe the behavior of soft interlayers with varying water content. Other researchers have focused on developing damage constitutive models that incorporate the effects of rock-water interactions and cyclic wetting-drying (Yu et al., 2024). Liu et al. (2024) developed a time-dependent expansion model for mudstone submerged in water, based on rheological theory, while Ping et al. (2024) constructed a mechanical damage model to predict the behavior of gypsum-bearing mudstone under varying dissolution times. These models highlight the importance of considering both the instantaneous and time-dependent effects of water on the mechanical behavior of mudstone. Moreover, Yang et al. (2019) investigated deformation and failure of mudstone under triaxial compression using experiment and particle flow code, which can be significant for the design of deep tunnel support. Additionally, recent studies by Shao et al. (2024) and Zheng et al. (2024) have explored the influence of microstructure on the mechanical behavior of similar geomaterials, providing valuable insights into the damage mechanisms at play.

However, existing studies exhibit several limitations. First, the long-term creep behavior under multi-stage stress conditions, particularly in the presence of varying water content, requires further investigation. Second, the interaction between water content and confining pressure in controlling creep damage has not been fully explored. Third, existing constitutive models often simplify the damage evolution process and fail to comprehensively consider the microstructural degradation caused by water. These limitations hinder the accurate prediction of the long-term performance of mudstone in practical engineering applications. This study aims to systematically investigate the influence of water content on the short-term strength, elastic modulus, and creep behavior of mudstone, and to develop a creep damage model that incorporates the effects of water content.

2. Materials and method

2.1. Specimen preparation

The mudstone specimens used in this study were obtained from a slope excavation site. This site is located in a geological environment characterized by sedimentary rocks, and the mudstone specimens are representative of the local geological stratum. The mudstone samples present as maroon-colored, dense blocks. The surface exhibits a soil-like texture, and microscopic observation reveals a silt-like structure. The average unit weight of the natural rock is approximately $2260\,\mathrm{kg/m^3}$, indicating a relatively high density compared to other sedimentary rock types.

All specimens were prepared as standard cylindrical specimens, adhering strictly to the guidelines of the International Society for Rock Mechanics (Bieniawski & Bernede, 1979). Initially, the mudstone blocks were cut into approximate cylindrical shapes using a diamond-wire saw. Subsequently, the specimens were polished using a grinding machine to ensure dimensional precision. The final specimens had a diameter of 50 mm and a height of 100 mm. To ensure the accuracy of the experimental results, the flatness of the end surfaces of each specimen was controlled to within 0.03 mm. This high-precision preparation minimizes the influence of specimen geometry and surface roughness on the experimental results, thus ensuring the reliability of the subsequent mechanical property tests. The detailed parameters of each specimen are shown in Table 1.

Specimen number	Water content [%]	Diameter [mm]	Height [mm]	Weight [g]	Density [g/cm ³]
uc01	0.00	50.01	100.04	443.68	2.26
uc02	0.26	49.69	99.77	442.53	2.29
uc03	0.72	49.92	100.08	441.44	2.25
uc04	1.64	50.02	100.16	442.32	2.25
cr-01	0.00	49.87	100.24	445.44	2.28
cr-02	0.26	49.88	100.46	442.71	2.26
cr-03	0.72	49.75	102.42	442.72	2.22
cr-04	1.64	50.01	99.79	445.52	2.27

Table 1. Specimens parameters.

2.2. Determination of water content

The water content of the mudstone specimens was controlled by oven drying and vacuum saturation methods. First, the natural mudstone specimens were weighed and then placed in an oven at $105\,^{\circ}$ C for 24 hours for complete drying, after which they were weighed again. Subsequently, portions of the dried specimens were vacuum-saturated in a vacuum saturator for a minimum of 12 hours to determine the saturated water content. Additional specimens were immersed in deionized water for 3 hours and 6 hours to achieve intermediate water contents. In this experiment, four distinct water content levels were employed: $0\,\%$ (dry), $0.26\,\%$, $0.72\,\%$, and $1.64\,\%$ (saturated), as indicated in Table 1.

2.3. Testing apparatus and procedure

2.3.1. Testing apparatus

The uniaxial compression tests were performed using a TFD-2000 electro-hydraulic servo rock triaxial testing machine (Fig. 1). This machine is capable of acquiring high- and low-speed data with excellent dynamic response, static stability, and system stiffness. The maximum axial load capacity is 2000 kN, and the maximum confining pressure and pore pressure are 100 MPa, with an accuracy of 0.1 %. The system comprises an axial loading system, a fluid pressure loading system (for water and confining pressure), a data acquisition system, and a central control system. The machine is capable of performing uniaxial compression, triaxial compression, seepage, creep, direct tensile, and indirect tensile tests, and it can synchronously record stress-strain curves throughout the rock loading process.

2.3.2. Testing procedure

A series of step-loading creep tests were conducted on mudstone specimens with different water contents, as summarized in Table 2. The load levels for each step were determined as 20%, 35%, 50%, 65%, and 80% of the uniaxial compressive strength of mudstone at the corresponding



Fig. 1. TFD-2000 electro-hydraulic servo rock triaxial testing machine.

Specimen number	Water content [%]	σ_c [MPa]	1st stage load [MPa]	2nd stage load [MPa]	3rd stage load [MPa]	4th stage load [MPa]	5th stage load [MPa]
cr-01	0.00	1.43	0.286	0.50	0.72	0.93	1.14
cr-02	0.26	0.77	0.154	0.27	0.39	0.50	0.62
cr-03	0.72	0.56	0.112	0.20	0.28	0.36	
cr-04	1.64	0.44	0.088	0.15	0.22		

Table 2. Step-loading values for creep tests.

water content. During the test, each load level was applied at a loading rate of $0.5\,\mathrm{MPa/s}$ until reaching the designated value, and then maintained for 48 hours.

After the 48-hour creep period at each load level, the specimens were carefully examined. If no signs of failure, such as a significant increase in the deformation rate or visible cracks on the specimen surface, were observed, the experiment proceeded to the next loading stage. However, if the specimens exhibited a significant increase in the deformation rate, indicating the onset of the accelerating creep stage and imminent bearing capacity loss, or if visible cracks appeared on the specimen surface, signifying severe damage to the internal structure, the specimens were considered to have experienced creep failure, and the test was terminated. This experimental procedure ensured the accurate investigation of the creep behavior of mudstone under different water content and stress conditions, providing reliable data for subsequent analysis of the long-term mechanical properties of mudstone.

3. Test results and analysis

3.1. Short-term strength

Prior to the long-term experiments, a series of uniaxial compression tests were performed on mudstone specimens with varying water contents. The resulting stress-strain curves are presented in Fig. 2.

A comparison of the post-peak stress-strain curves of specimens with different water contents reveals a distinct influence of water content on the mechanical behavior of mudstone. Under lower water content conditions, the rock specimens exhibit characteristic brittle behavior. Upon reach-

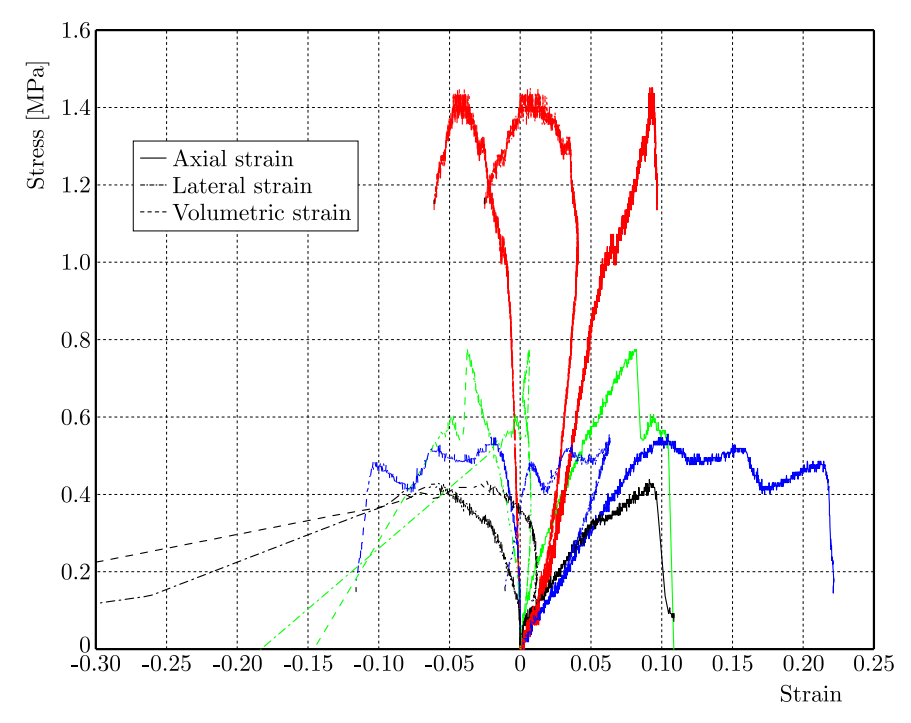


Fig. 2. Stress-strain curves of mudstone under different water content.

ing the peak stress, abrupt failure of the internal structure occurs due to the rapid accumulation of internal stress. The specimen fails suddenly, and the stress drops precipitously, indicating an almost instantaneous loss of bearing capacity. Conversely, under higher water content conditions, the brittleness of the mudstone is reduced, and the behavior becomes more plastic. After reaching the peak stress, the specimen can sustain a certain amount of deformation without immediate failure. This is attributed to the water-lubricated particles' ability to adjust their positions, dissipating the energy of external forces through plastic deformation. Consequently, the stress-strain curve exhibits a more gradual decline, indicating that the specimen retains some capacity to resist further deformation after the peak stress.

Figure 3 illustrates the relationship between uniaxial compressive strength, elastic modulus, and water content for the mudstone specimens. As the water content increases, both the uniaxial

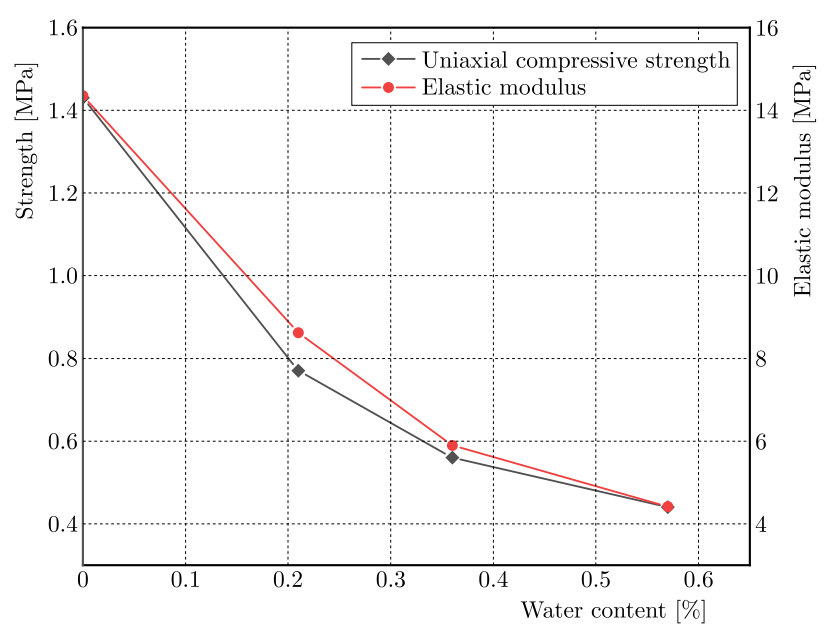


Fig. 3. Uniaxial compressive strength and elastic modulus vs water content.

compressive strength and elastic modulus of the mudstone decrease continuously. The initial uniaxial compressive strength of the dry mudstone specimen was $1.43\,\mathrm{MPa}$, while at a water content of $1.64\,\%$ (saturation), the strength decreased to $0.44\,\mathrm{MPa}$, representing a reduction of $69.45\,\%$. Similarly, the elastic modulus decreased significantly with increasing water content, from $14.35\,\mathrm{MPa}$ for the dry specimen to $4.12\,\mathrm{MPa}$ for the saturated specimen, a reduction of $69.23\,\%$. To quantify the statistical significance of the observed trends, a one-way ANOVA was performed on the uniaxial compressive strength and elastic modulus data. The results indicated a statistically significant effect of water content on both parameters (p < 0.05). Post-hoc tests (Tukey's HSD) revealed significant differences between the strength and modulus values at different water content levels.

Statistical analysis of the uniaxial compressive strength and elastic modulus data revealed an exponential decline in both properties with increasing water content. The relationships between these properties and water content were fitted to derive specific expressions. These expressions can be used to predict the uniaxial compressive strength and elastic modulus of mudstone under different water content conditions, providing a valuable tool for engineering design.

3.2. Creep behavior of mudstone under different water content

The uniaxial creep curves of mudstone under different water content conditions are shown in Fig. 4. At low water content, the creep deformation of mudstone is relatively small. The creep rate decreases rapidly during the primary creep stage. This behavior is attributed to the relatively stable internal structure of mudstone at low water content. The particles are tightly bound, and the resistance to deformation is high. The specimen exhibits some elastic-like behavior, and creep deformation is primarily due to elastic-recovery-like adjustments within the internal structure of the mudstone under external stress.

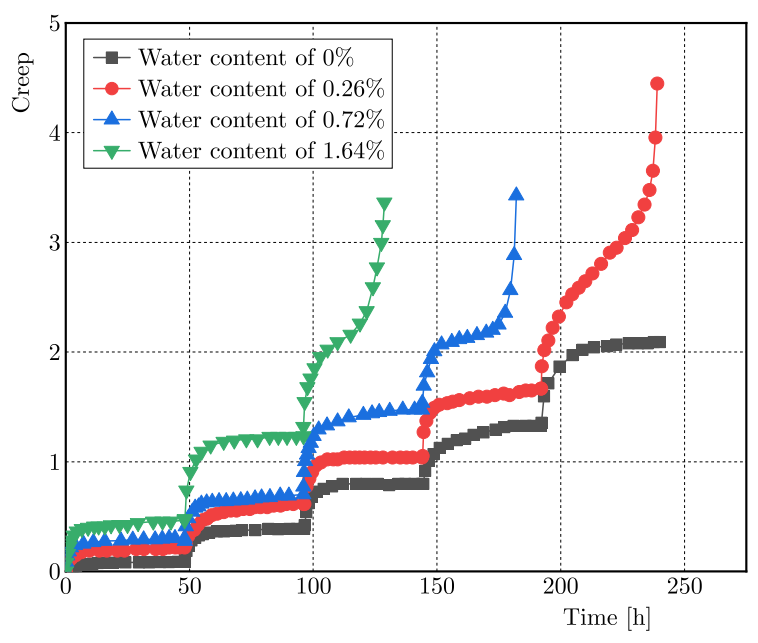


Fig. 4. Uniaxial creep curves of mudstone under different water contents.

As the water content increases, the creep deformation of mudstone increases significantly, and the primary creep stage becomes shorter. This is because the increase in water content leads to the softening of the mudstone. Water in the pores further lubricates the particles, reducing friction between them. The internal structure of the mudstone becomes looser, facilitating particle movement and rearrangement under external stress. As a result, the specimen enters the secondary creep stage earlier. In the secondary creep stage, although the creep rate becomes relatively stable, the overall creep deformation is much greater than that at low water content.

For specimens with different water contents, the creep curves share common characteristics yet also display differences. Figures 5, 6, and 7 all illustrate the three-stage creep process: decelerating (primary) creep, steady-state (secondary) creep, and accelerating (tertiary) creep. However, due to varying water contents and applied loads, their behaviors differ. The specimen with 0.26 % water content under a load of 0.616 MPa, the one with 0.72 % water content under 0.364 MPa, and the 1.64% water-content specimen under 0.22 MPa all start with a decelerating creep stage where the creep rate decreases rapidly as the internal structure adjusts to the load. This is followed by the steady-state creep stage with a relatively stable creep rate. Finally, they enter the accelerating creep stage as the internal structure deteriorates. The specimen with a higher water content generally shows a shorter overall creep-time-to-failure. For example, the 1.64 % water-content specimen reaches the accelerated creep stage and fails more quickly

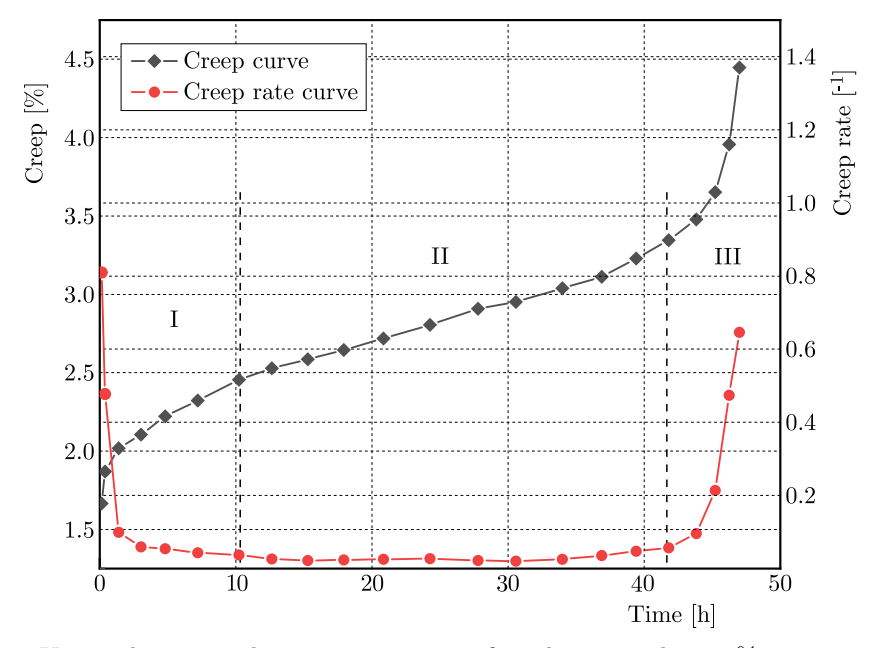


Fig. 5. Uniaxial creep and creep rate curves of mudstone with $0.26\,\%$ water content under the fifth-stage load of $0.616\,\mathrm{MPa}$.

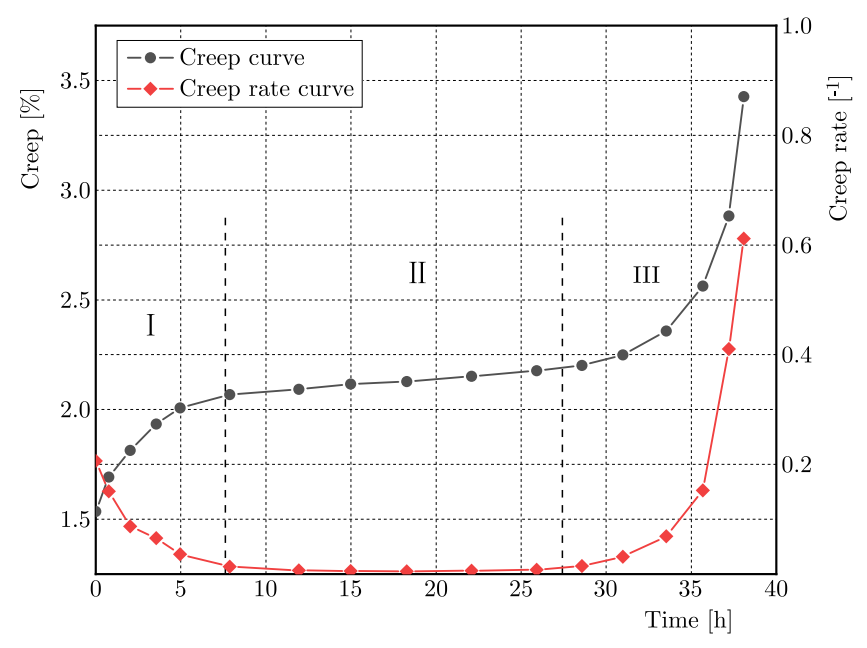


Fig. 6. Uniaxial creep and creep rate curves of mudstone with $0.72\,\%$ water content under the fourth-stage load of $0.364\,\mathrm{MPa}$.

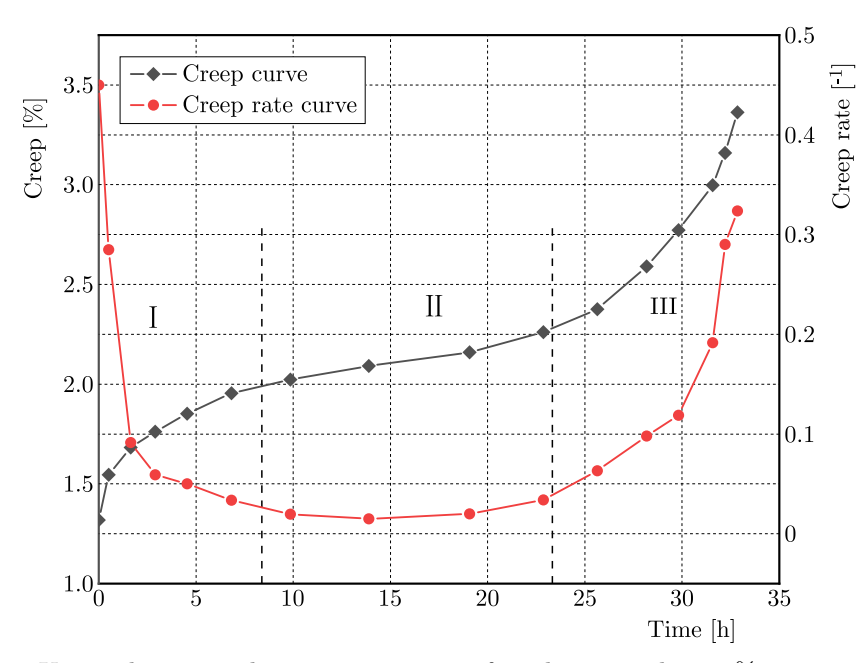


Fig. 7. Uniaxial creep and creep rate curves of mudstone with $1.64\,\%$ water content under the third-stage load of $0.22\,\mathrm{MPa}$.

compared to the 0.26% and 0.72% water-content specimens, indicating that water content significantly influences the creep failure time and overall creep behavior of mudstone.

4. Creep damage constitutive model

4.1. Burgers creep model

The Burgers creep model is a widely used mechanical model in rock mechanics, which can effectively describe the complex creep behavior of rocks. It is composed of a Maxwell body and a Kelvin body connected in series (Yang et al., 2023), as shown in Fig. 8, and the creep equation is

$$\varepsilon(t) = \frac{\sigma}{E_1} + \frac{\sigma}{\eta_1} t + \frac{\sigma}{E_2} \left(1 - e^{-\frac{E_2}{\eta_2} t} \right),\tag{4.1}$$

where σ and ε are stress and strain; E_1 and η_1 are the elastic modulus and viscosity coefficient of the Maxwell body; and E_2 , η_2 are the elastic modulus and viscosity coefficient of the Kelvin body.

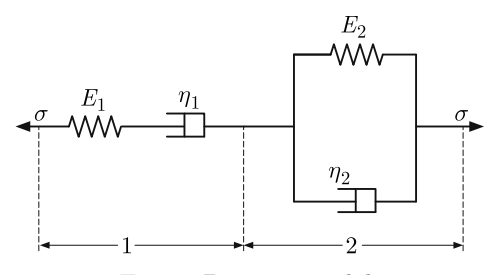


Fig. 8. Burgers model.

However, the Burgers creep model has several inherent limitations (Goodman, 2008; Jaeger & Cook, 2007). Composed of linear elements (a spring-dashpot series in the Maxwell body and a spring-dashpot parallel combination in the Kelvin body), it cannot accurately represent the

accelerating creep stage. The rapid increase in the deformation rate during this stage is a non-linear behavior that the model's linear components cannot capture, which leads to inaccuracies in predicting full-range creep.

For mudstone, which is highly sensitive to water content changes, the Burgers model fails to account for internal damage evolution (Hudson & Harrison, 1997; Brown, 2004). It does not consider how water-induced micro-structural degradation affects the creep process (Hoek & Brown, 2002; Lemaitre, 1996). Water infiltration softens clay minerals in mudstone, causing water-induced damage and altering its internal structure, but the Burgers model cannot incorporate these changes.

As a result, the model cannot adequately describe the weakening of mudstone's mechanical properties due to water-rock interactions, which limits its accuracy in predicting long-term behavior under different water contents. To address these issues, it is very necessary to define water-induced and creep-induced damage variables.

4.2. Damage variable

Based on damage mechanics theory, the damage variable is defined as the ratio of the defective area of the material to the total effective load-bearing area of the material (Murakami, 1988; Kachanov, 1958). Mathematically, it can be expressed as

$$D = \frac{A_0 - A_w}{A_0} = 1 - \frac{A_w}{A_0},\tag{4.2}$$

where A_0 is the effective bearing area in the undamaged state, and A_w is the effective bearing area in the damaged state due to the influence of water content.

As shown in Subsection 3.1, the elastic modulus of mudstone follows an exponential decay with the increase in water content. The fitting equation for the elastic modulus E and water content w can be expressed as

$$E_w = E_0 e^{-fw}, (4.3)$$

where E_0 is the elastic modulus of the dry mudstone specimen, and f and w are fitting parameters.

Since the elastic modulus is related to the effective load-bearing area of the material, and the change in elastic modulus with water content reflects the degree of damage to the material caused by water, when the material is damaged by water, the elastic modulus decreases. According to the definition of the damage variable, the water-content-induced damage variable D_w can be expressed as

$$D_w = 1 - \frac{E(w)}{E_0} = 1 - e^{-fw}. (4.4)$$

Meanwhile, mudstone is also affected by creep during long-term service. The creep-induced damage of mudstone is a process of continuous internal structure degradation over time (Rabotnov, 1969; Lemaitre & Chaboche, 1990). In the study of creep-induced damage, we start from the basic concept of damage mechanics. The damage variable is often defined to describe the degree of material degradation.

Let us assume that the rate of damage evolution $\frac{dD_c}{dt}$ is proportional to a power-law function of time. Mathematically, it can be written as

$$\frac{\mathrm{d}D_c}{\mathrm{d}t} = kt^{n-1},\tag{4.5}$$

where k is a proportionality constant and n is a material-specific parameter.

Integrating both sides of the equation with respect to time from 0 to t (Rabotnov, 1969; Lemaitre & Chaboche, 1990):

$$\int_{0}^{D_{c}} dD_{c} = \int_{0}^{t} kt^{n-1} dt, \qquad D_{c} = k \frac{t^{n}}{n} \Big|_{0}^{t}, \qquad D_{c} = \frac{k}{n} t^{n}.$$
(4.6)

Considering the physical meaning that at t=0, $D_c=0$, and normalizing the damage variable so that D_c ranges from 0 (undamaged) to 1 (completely damaged), after a series of mathematical treatments and in combination with a large number of experimental studies and theoretical analyses, we can assume that $D_c=1-e^{-t^n}$. This parameter n can be determined by conducting a series of creep tests on mudstone specimens, and then fitting the experimental data of the creep-induced damage degree changing with time, so as to accurately reflect the development law of creep-induced damage of mudstone.

Considering both the damage caused by water content and creep, the total damage variable, D of mudstone can be expressed as a combination of the two damage variables (Krajcinovic, 1996):

$$D = 1 - (1 - D_w)(1 - D_c). (4.7)$$

This formula comprehensively considers the coupling effect of water-content-induced damage and creep-induced damage on mudstone. As the water content w increases, the value of e^{-fw} decreases, and D_w increases, indicating that the degree of damage to the mudstone caused by water becomes more severe. And as the creep time t increases, the value of e^{-t^n} decreases, and D_c increases, reflecting the continuous development of creep-induced damage. This comprehensive damage variable equation provides a more accurate and comprehensive basis for further establishing the creep damage constitutive model considering the influence of water content, which can more accurately describe the mechanical behavior of mudstone under different water content and creep-time conditions.

4.3. Creep damage constitutive model

To establish a creep damage constitutive model that takes into account the influence of water content and creep behavior (Krajcinovic, 1996), we combine the Burgers model with the damage variable. Figure 9 illustrates the proposed creep damage model, which integrates the Burgers model with both water-induced and creep-induced damage variables. This integration allows a more comprehensive representation of the complex interactions that govern the long-term behavior of mudstone.

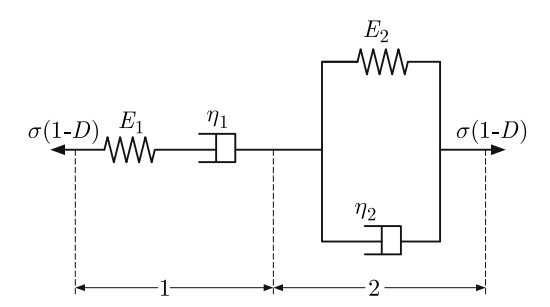


Fig. 9. Illustration of the creep damage model.

The total strain of the mudstone considering damage can be expressed as

$$\varepsilon(t) = (1 - D)\frac{\sigma}{E_1} + \frac{\sigma}{\eta_1}t + \frac{\sigma}{E_2}\left(1 - e^{-\frac{E_2}{\eta_2}t}\right). \tag{4.8}$$

4.4. Model verification

To verify the accuracy and reliability of the established creep damage model, we compared the model's calculated results with our experimental data. Due to the limited number of specimens tested under creep conditions, we selected all creep test specimens for model calibration and validation. This approach maximizes the use of available data to assess the model's performance. The fitting process employed the Quasi-Newton (BFGS) method. We selected several representative specimens with different water contents from the experiment and input the corresponding stress levels and material parameters into the model. Then, we calculated the creep strain at different times using the model and compared it with the measured creep strain from the experiment. The results of this comparison are visually presented in Fig. 10.

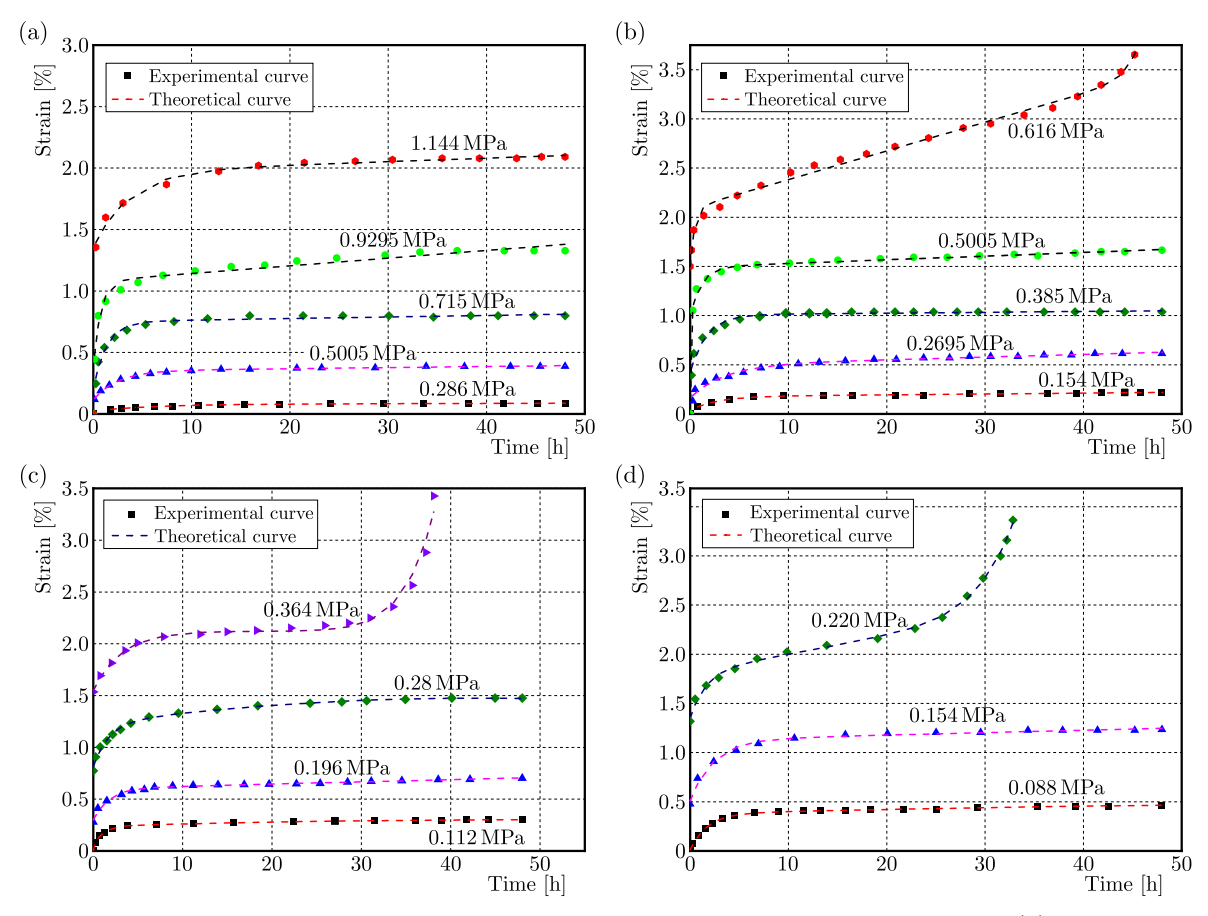


Fig. 10. Comparison between experimental creep curves and creep damage model curves: (a) water content of 0.00%; (b) water content of 0.26%; (c) water content of 0.72%; (d) water content of 1.64%.

It can be seen from Fig. 10 that the experimental creep curves and the curves simulated by the proposed creep damage model for specimens with different water contents demonstrate a reasonable degree of agreement. The experimental data points are plotted as discrete markers, while the model-predicted curves are shown as continuous lines. Specifically, during the primary creep stage, the model-predicted curves accurately capture the decreasing trend of the creep rate, aligning with the experimental observations. During the secondary creep stage, the predicted creep rates are close to the measured values, indicating that the model can effectively represent the relatively stable creep behavior. In the tertiary creep stage, although minor discrepancies exist between the model-predicted and experimental curves, the model still reflects the overall trend of accelerating creep deformation. The parameters used for the model fitting are listed in Table 3. These parameters were obtained through the fitting process and are specific to each specimen's water content and stress level. This overall agreement between model predictions and

Water content [%]	Stress [MPa]	E_1 [MPa]	$\begin{array}{c} \eta_1 \\ [\text{MPa} \cdot \text{h}] \end{array}$	E_2 [MPa]	$\frac{\eta_2}{[\text{MPa} \cdot \text{h}]}$	f	n	k	R^2
0	0.29	13.51	1335.45	5.13	28.46	0.00	24.94	0.00	0.99
	0.50	4.41	546.32	2.12	5.09	0.00	19.21	0.00	1.00
	0.72	23.83	345.17	1.03	0.78	0.00	66.20	0.00	0.98
	0.93	2.57	149.10	1.29	0.94	0.00	30.34	0.00	0.97
	1.14	0.85	406.13	1.86	6.59	0.00	72.17	0.00	0.99
0.26	0.15	1.19E-04	10.00	3.03E-05	9.04E-05	40.087	2.454	-3.14E-05	0.99
	0.27	0.92	10.00	0.46	0.87	2.938	1.012	0.01	0.99
	0.39	4.21E-03	0.32	2.97E-03	3.67E-03	20.945	2.045	1.12E-04	0.98
	0.50	6.83E-03	5.25	109.14	2.31	14.704	-0.491	-8.54E-02	1.00
	0.62	1.16E-02	0.58	2.69E-02	1.11E-02	13.810	35.973	-7.24E-60	1.00
0.72	0.11	1.28	17.11	0.31	0.32	0.90	1.17	3.15E-03	1.00
	0.20	1.40	191.45	1.37	2.30	-1.05	20.77	0.00	0.99
	0.28	0.42	20.47	0.84	1.42	-0.28	1.18	3.38E-03	0.99
	0.36	2.87E-05	45482.50	7.74E-05	2.44E-04	12.52	11.50	-4.10E-18	0.98
1.64	0.09	1.92E-03	2.49	6.68E-05	1.19E-04	4.98	1.00	-4.45E-03	1.00
	0.15	0.29	59.85	0.24	0.57	2.58E-02	88.58	0.00	0.99
	0.22	0.16	11.81	0.48	0.74	-2.54E-04	8.85	-1.27E-13	1.00

Table 3. Parameters of the creep damage constitutive model.

experimental measurements, despite some simplifications in the model and potential measurement errors in the experimental data, supports the effectiveness of the proposed creep damage model in describing the creep behavior of mudstone under different water content and stress conditions.

5. Conclusion

This study has comprehensively investigated the long-term mechanical properties of mudstone under different water content conditions. The results have demonstrated that water content has a significant impact on the short-term strength, elastic modulus, and creep behavior of mudstone.

In terms of short-term strength, both the uniaxial compressive strength and elastic modulus of mudstone decrease exponentially with increasing water content. The initial uniaxial compressive strength of dry mudstone was 1.43 MPa, and it dropped to 0.44 MPa when the water content reached 1.64 % (saturation), with a reduction of 69.45 %. The elastic modulus decreased from 14.35 MPa for the dry specimen to 4.12 MPa for the saturated specimen, a reduction of 69.23 %. This exponential decline indicates that water has a strong softening effect on mudstone, which should be carefully considered in engineering designs.

Regarding the creep behavior, water content also plays a crucial role. When the water content is low, the creep deformation of mudstone is relatively small, and the specimen shows some elastic-like behavior in the primary creep stage. However, as the water content increases, the creep deformation increases significantly, the primary creep stage becomes shorter, and the specimen enters the secondary creep stage earlier. Higher water content accelerates the creep failure of mudstone, which poses potential risks to the long-term stability of engineering projects.

To better understand the long-term mechanical behavior of mudstone under varying water content conditions, we proposed expressions for water-induced and creep-induced damage variables and developed a creep damage model based on the combination of these damage variables and the Burgers creep model. This model can effectively describe the complex creep behavior of mudstone. The verification results showed that the model-calculated values were in good agreement with the experimental data, although there were some errors due to model simplification and experimental measurement errors.

Future research could focus on further improving the model by considering more complex factors such as the interaction between water and other chemical substances in mudstone, as well as the influence of different stress states on creep damage. Additionally, more advanced experimental techniques can be employed to accurately measure the micro-structural changes of mudstone during the creep process, which will help to establish more accurate constitutive models and provide more reliable theoretical support for engineering applications.

References

- 1. Bieniawski, Z.T., & Bernede, M.J. (1979). Suggested methods for determining the uniaxial compressive strength and deformability of rock materials. *International Journal of Rock Mechanics and Mining Sciences & Geomechanics Abstracts*, 16(2), 135–140.
- 2. Brown, E.T. (2004). Rock characterization, testing and monitoring: ISRM suggested methods. ISRM.
- 3. Chen, F., Sun, X., & Lu, H. (2022). Influence of water content on the mechanical characteristics of mudstone with high smectite content. *Geofluids*, 2022(1), Article 9855213. https://doi.org/10.1155/2022/9855213
- Gao, Y., Wei, W., & Jiang, Q. (2023). Effect of water content on mechanical properties and internal microcrack evolution in mudstone. Arabian Journal for Science and Engineering, 48(10), 12775— 12791. https://doi.org/10.1007/s13369-022-07569-9
- 5. Goodman, R.E. (2008). Introduction to rock mechanics (2nd ed.). John Wiley & Sons.
- Hoek, E., & Brown, E.T. (1997). Practical estimates of rock mass strength. International Journal of Rock Mechanics and Mining Sciences, 34(8), 1165–1186. https://doi.org/10.1016/S1365-1609(97)80069-X
- 7. Hudson, J.A., & Harrison, J.P. (1997). Engineering rock mechanics: an introduction to the principles. Elsevier.
- 8. Jaeger, J.C., Cook, N.G.W., & Zimmerman, R.W. (2007). Fundamentals of rock mechanics (4th ed.). Blackwell Publishing.
- 9. Kachanov, L.M. (1958). Time of the rupture process under creep conditions. *Izvestiia Akademii Nauk SSSR*, Otdelenie Teckhnicheskikh Nauk, 8, 26–31.
- 10. Krajcinovic, D. (1996). Damage mechanics. Elsevier.
- 11. Lemaitre, J. (1996). A course on damage mechanics. Springer. https://link.springer.com/book/ 10.1007/978-3-642-18255-6
- 12. Lemaitre, J., & Chaboche, J.L. (1990). *Mechanics of solid materials*. Cambridge University Press. https://docs.dicatechpoliba.it/filemanager/407/MECHANICS%20OF%20SOLID%20MATERIALS %20-%20cap%201%20e%203.pdf
- 13. Li, J., Gao, Y., Yang, T., Zhang, P., Deng, W., & Liu, F. (2023). Effect of water on the rock strength and creep behavior of green mudstone. Geomechanics and Geophysics for Geo-Energy and Geo-Resources, 9(1), Article 101. https://doi.org/10.1007/s40948-023-00638-9
- 14. Liu, C.-D., Cheng, Y., Jiao, Y.-Y., Zhang, G.-H., Zhang, W.-S., Ou, G.-Z., & Tan, F. (2021). Experimental study on the effect of water on mechanical properties of swelling mudstone. *Engineering Geology*, 295, Article 106448. https://doi.org/10.1016/j.enggeo.2021.106448
- 15. Liu, J., Zhang, Q., Wang, L., Chen, F., Wang, P., Yan, X., & Guo, L. (2024). A time-dependent expansion model for mudstone submerged in water. *Soil Mechanics and Foundation Engineering*, 61(1), 20–26. https://doi.org/10.1007/s11204-024-09938-y

 Ma, C., Zhan, H.-B., Yao, W.-M., & Li, H.-Z. (2018). A new shear rheological model for a soft interlayer with varying water content. Water Science and Engineering, 11(2), 131–138. https://doi.org/ 10.1016/j.wse.2018.07.003

- 17. Murakami, S. (1988). Mechanical modeling of material damage. *Journal of Applied Mechanics (ASME Transactions)*, 55(2), 280–286. https://doi.org/10.1115/1.3173673
- 18. Ping, S., Wang, F., Wang, D., Li, S., Wang, Y., Yuan, Y., & Feng, G. (2024). Mechanical damage induced by the water–rock reactions of gypsum-bearing mudstone. *Rock Mechanics and Rock Engineering*, 57(8), 6377–6394. https://doi.org/10.1007/s00603-024-03855-0
- 19. Qi, S., Zhang, H., Bian, H., Wang, J., Xu, S., & Wu, B. (2024). Damage characteristics and degradation mechanism of silty mudstone under wet–dry cycling. *Geotechnical and Geological Engineering*, 42(7), 6095–6112. https://doi.org/10.1007/s10706-024-02877-3
- 20. Rabotnov, Yu.N. (1969). Creep problems in structural members. North-Holland Publishing Company.
- 21. Sawatsubashi, M., Kiyota, T., & Katagiri, T. (2021). Effect of initial water content and shear stress on immersion-induced creep deformation and strength characteristics of gravelly mudstone. *Soils and Foundations*, 61(5), 1223–1234. https://doi.org/10.1016/j.sandf.2021.06.015
- 22. Schimmell, M.T.W., Hangx, S.J.T., & Spiers, C.J. (2022). Effect of pore fluid chemistry on uni-axial compaction creep of Bentheim sandstone and implications for reservoir injection operations. Geomechanics for Energy and the Environment, 29, Article 100272. https://doi.org/10.1016/j.gete.2021.100272
- 23. Shao, Z., Song, Y., Zheng, J., Shen, F., Liu, C., & Yang, J. (2024). Damage degradation mechanism and macro-meso structural response of mudstone after water wetting. *Journal of Mountain Science*, 21(8), 2825–2843. https://doi.org/10.1007/s11629-023-8580-x
- 24. Wang, J.-G., Sun, Q.-L., Liang, B., Yang, P.-J., & Yu, Q.-R. (2020). Mudstone creep experiment and nonlinear damage model study under cyclic disturbance load. *Scientific Reports*, 10, Article 9305. https://doi.org/10.1038/s41598-020-66245-w
- 25. Wang, Y., Cong, L., Yin, X., Yang, X., Zhang, B., & Xiong, W. (2021). Creep behaviour of saturated purple mudstone under triaxial compression. *Engineering Geology*, 288, Article 106159. https://doi.org/10.1016/j.enggeo.2021.106159
- Yang, S.-Q., Tian, W.-L., Jing, H.-W., Huang, Y.-H., Yang, X.-X., & Meng, B. (2019). Deformation
 and damage failure behavior of mudstone specimens under single-stage and multi-stage triaxial compression. Rock Mechanics and Rock Engineering, 52(3), 673–689. https://doi.org/10.1007/s00603018-1622-y
- 27. Yang, Y.-L., Zhang, T., Liu, S.-Y., & Luo, J.-H. (2022). Mechanical properties and deterioration mechanism of remolded carbonaceous mudstone exposed to wetting-drying cycles. *Rock Mechanics and Rock Engineering*, 55(6), 3769–3780. https://doi.org/10.1007/s00603-022-02833-8
- 28. Yang, Y.J., Huang, G., Zhang, Y.Q., & Yuan, L. (2023). An improved Burgers creep model of coal based on fractional-order. Frontiers in Earth Science, 11, Article 1277147. https://doi.org/10.3389/feart.2023.1277147
- 29. Yu, X.-W., Fu, H.-Y., Zeng, L., Liu, J., & Qiu, X.-Y. (2024). Damage constitutive model for soft rocks and its experimental verification on silty mudstone considering cyclic rock-water interactions. *Bulletin of Engineering Geology and the Environment*, 83(6), Article 254. https://doi.org/10.1007/s10064-024-03740-8
- 30. Zheng, J., Song, Y., Shen, F., Shao, Z., Liu, C., & Yang, J. (2024). Study on mechanical properties of water-immersed mudstone based on nanoindentation tests. *Mining, Metallurgy & Exploration*, 41(4), 2031–2046. https://doi.org/10.1007/s42461-024-01027-w
- 31. Zou, J., Li, G., Li, Z., Zhang, Y., Liu, H., & Wang, Y. (2024). Experimental study on the mechanical characteristics of weakly cemented mudstone under different loading rates. *Scientific Reports*, 14, Article 15364. https://doi.org/10.1038/s41598-024-65024-1